



PUBLISHED FOR SISSA BY SPRINGER

RECEIVED: May 22, 2011

REVISED: July 7, 2011

ACCEPTED: July 14, 2011

PUBLISHED: August 5, 2011

Magnetized domain walls in the deconfined Sakai-Sugimoto model at finite Baryon density

Piyabut Burikham^{a,b,c} and Tossaporn Chullaphan^a

^a*Theoretical High-Energy Physics and Cosmology Group, Department of Physics,
Faculty of Science, Chulalongkorn University,
Phyathai Road, Bangkok 10330, Thailand*

^b*Thailand Center of Excellence in Physics, CHE, Ministry of Education,
Bangkok 10400, Thailand*

^c*Department of Physics, CERN Theory Division,
CH-1211 Geneva 23, Switzerland*

E-mail: piyabut@gmail.com, chullaphan.t@gmail.com

ABSTRACT: The magnetized pure pion gradient ($\nabla\varphi$) phase in the deconfined Sakai-Sugimoto model is explored at zero and finite temperature. We found that the temperature has very small effects on the phase. The thermodynamical properties of the phase show that the excitations behave like scalar solitonic free particles. By comparing the free energy of the pion gradient phase to the competing multiquark-pion gradient (MQ- $\nabla\varphi$) phase, it becomes apparent that the pure pion gradient is less thermodynamically preferred than the MQ- $\nabla\varphi$ phase. However, in the parameter space where the baryonic chemical potential is smaller than the onset value of the multiquark, the dominating magnetized nuclear matter is the pion gradient phase.

KEYWORDS: Holography and quark-gluon plasmas, Brane Dynamics in Gauge Theories, D-branes

ARXIV EPRINT: [1105.2729](https://arxiv.org/abs/1105.2729)

Contents

1	Introduction	1
2	Holographic setup of the magnetized chirally broken phase	2
2.1	Zero temperature approximation $f(u) \simeq 1$	5
3	Thermodynamical properties of the pure pion gradient phase	8
3.1	Comparison to the multiquark- $\nabla\varphi$ phase	12
4	Conclusions and discussions	13

1 Introduction

Physics of dense nuclear matter is one of the most challenging area due to the lack of appropriate theoretical modeling. On one hand, the entities in the nuclear matter strongly couple to one another and therefore the perturbative treatment cannot be applied in a straightforward manner. On the other hand, the lattice approach to the Quantum Chromodynamics (QCD) can be applied to the situations of hot nuclear matter. The lattice results predict the deconfinement phase transition at temperature around 175 MeV for the dilute nuclear matter. However, this approach also faces difficulty in describing the nuclear matter with finite density due to the fermion sign problem.

An alternative and complementary approach is the application of the holographic principle or the AdS/CFT correspondence [1–3] to study the properties of the nuclear matter. The Sakai-Sugimoto (SS) model [4, 5] is a holographic model which could approximate the QCD at low energy most accurately. Starting with a type IIA string background with D4-branes as the source. Take the near-horizon limit and add the black hole horizon to generate Hawking-Page temperature to be identified with the temperature of the dual gauge matter. Since we need an approximately 4 dimensional QCD, one of the 5 dimensional sub-space is compactified into a circle whose radius is chosen so small that the Kaluza-Klein states are much heavier than the relevant energy scales and temperatures.

The quarks and antiquarks are introduced as open-string excitations on the stack of N_f flavour D8 and $\overline{D8}$ branes located at fixed separation distance in the compactified coordinate. The boundary conditions of the sparticles in the circle are chosen to be antisymmetric at the location of the flavour branes and the zeroth modes are thus eliminated. Consequently, the gauge theory at the flavour branes is a SUSY-broken 5 dimensional Yang-Mills theory with quarks and antiquarks in the fundamental representation. The effective theory has the same particle content as the QCD. Using the AdS/CFT correspondence, the bulk theory of this brane configuration is conjectured to be dual to the QCD-like gauge theory at the boundary. The striking feature of the SS model is that it provides a natural geometric realization of the chiral symmetry breaking. When the D8 and $\overline{D8}$ merge at certain location

in the radial coordinate, the quarks and antiquarks do not transform independently under the chiral transformation and therefore the chiral symmetry is broken in the connected brane configuration. A chiral symmetric configuration occurs when the two flavour branes are parallel and the dual gauge matter will be in the chiral symmetric phase.

Subsequent investigation reveals that the SS model accommodates the exotic possibility that the chiral symmetry restoration and the deconfinement can occur separately [6] when the distance between the D8 and $\overline{D8}$ branes in the compactified dimension is not too large. The deconfinement could occur at relatively low temperature while the chiral symmetry would be restored at larger temperature. Even though both the chiral symmetry breaking and the confinement are results of the strong coupling of the gauge theory, they are independent of one another as far as we know. It is thus possible that the real QCD also has distinctive chiral symmetry restoration and deconfinement.

Chiral condensate of the QCD-like dense matter is explored in ref. [7] using the Wess-Zumino-Witten induced anomalous term in the chiral perturbation theory and in ref. [8] using the bottom-up AdS/QCD based on the confined SS model. When the magnetic field is applied, the condensate will respond by developing a gradient in the direction of the applied field. This gradient also carries the baryonic charge density proportional to the applied field and the gradient of the condensate. Holographic studies of the chiral condensate response to the magnetic field is investigated in ref. [9] for the confined SS model. In ref. [10], the pure pion gradient phase is explored and compared with the chiral symmetric quark-gluon plasma phase in the zero temperature approximation of the deconfined SS model. In ref. [11], it is roughly compared with the mixed phase of the multi-quark-pion gradient (MQ- $\nabla\varphi$) using a zero-instanton limit of the multi-quark configuration. The preliminary results suggest that the pure pion gradient phase might be thermodynamically less preferred than the MQ- $\nabla\varphi$ phase. In this article, we perform a thorough investigation into the pure pion gradient phase at finite temperature as well as its thermodynamical comparison to the MQ- $\nabla\varphi$ in order to obtain a more definitive quantitative result. It is found that the pure pion gradient phase is insensitive to the change of temperature in the range $T = 0 - 0.16$. It is also shown that the pure pion gradient phase is generically less preferred than the MQ- $\nabla\varphi$ phase except when the baryon chemical potential is smaller than the onset value of the multi-quarks. In that region of the phase diagram, the dominating phase is the pure pion gradient.

The article is organized as the following. In section 2, we setup the holographic model of the magnetized chirally broken nuclear phase without an instanton. A zero temperature solution is obtained and relevant dual physical quantities as well as their relationships are discussed. Thermodynamical properties of the pure pion gradient phase at finite temperature and the comparison with the multi-quark phase are discussed in section 3. Section 4 concludes the article.

2 Holographic setup of the magnetized chirally broken phase

In the non-antipodal SS model, a stack of N_c D4-branes generates a curved 10 dimensional spacetime in type IIA string theory. The near-horizon limit of this background is then

taken and the black hole horizon is added by introducing the factor $f(u)$ [3, 12] into the background. The x^4 direction is compactified with certain radius to obtain an effective (1 + 3) dimensional subspace in the low energy limit. The resulting spacetime of the Sakai-Sugimoto model is in the form

$$ds^2 = \left(\frac{u}{R_{D4}}\right)^{3/2} (f(u)dt^2 + \delta_{ij}dx^i dx^j + dx_4^2) + \left(\frac{R_{D4}}{u}\right)^{3/2} \left(u^2 d\Omega_4^2 + \frac{du^2}{f(u)}\right)$$

$$e^\phi = g_s \left(\frac{u}{R_{D4}}\right)^{3/4}, \quad R_{D4}^3 \equiv \pi g_s N_c l_s^3,$$

where $f(u) \equiv 1 - u_T^3/u^3$, $u_T = 16\pi^2 R_{D4}^3 T^2/9$. T is the Hawking-Page temperature of the black hole which is identified with the temperature of the dual gauge matter at the boundary. R_{D4} is the curvature of the background which is generically different from the compactified radius R of the x^4 coordinate. ϕ is the dilaton field, a function of u in this background.

We then introduce stacks of N_f D8 and $\overline{D8}$ flavour branes with separation L_0 on the circle of compactified x^4 at the boundary $u \rightarrow \infty$. Open string excitations with one end on these branes behave like chiral “quarks” and “antiquarks” in the fundamental representation of the $U(N_f)$. In the brane configuration where D8 and $\overline{D8}$ are parallel, open-string excitations on each stack of branes transform independently under the chiral transformation and thus we have a chiral symmetric background. The dual gauge matter will be in the chiral symmetric phase. On the other hand, in the connecting brane configuration, chiral symmetry is broken at the tip and the corresponding gauge matter will be in the chirally broken phase [6].

To add the baryonic density to the boundary gauge matter, the non-normalizable mode of the a_0^V component of the $U(1) \subset U(N_f)$ field is turned on. The baryon chemical potential μ of the corresponding gauge matter is identified with the non-normalizable mode of the DBI gauge field at the boundary by [13]

$$\mu = a_0^V(u \rightarrow \infty). \tag{2.1}$$

To turn on the magnetic field, another component a_3^V is used as the vector potential generating the magnetic field. The direction of the magnetic field is chosen so that the vector potential is

$$a_3^V = Bx_2. \tag{2.2}$$

The Chern-Simons action in the background couples these two components to the third component a_1^A of the $U(1)$, generating the response to the external magnetic field. The response appears as the gradient of the chiral condensate along the direction of B at the boundary which is defined to be $a_1^A(u \rightarrow \infty) \equiv \nabla\varphi$. Here and henceforth, we will call $\nabla\varphi$ a pion gradient.

The DBI and the Chern-Simons actions are then given by

$$S_{D8} = \mathcal{N} \int_{u_c}^{\infty} du u^{5/2} \sqrt{1 + \frac{B^2}{u^3}} \sqrt{1 + f(u)(a_1^A)^2 - (a_0^V)^2 + f(u)u^3 x_4'^2}, \quad (2.3)$$

$$S_{CS} = -\frac{3}{2} \mathcal{N} \int_{u_c}^{\infty} du (\partial_2 a_3^V a_0^V a_1^A - \partial_2 a_3^V a_0^V a_1^A), \quad (2.4)$$

where $\mathcal{N} = N_c R_{D4}^2 / (6\pi^2 (2\pi\alpha')^3)$ defines the brane tension. The factor $3/2$ in the Chern-Simons action comes from addition of surface term in order to maintain the gauge invariance of the total action in the situation when the gauge transformation does not vanish at the boundary (see ref. [9] for details). The integration limit u_c is the position of the tip of the D8-branes where it connects with the $\overline{D8}$.

Consequently, the equations of motion with respect to each gauge field a_0^V, a_1^A are

$$\frac{\sqrt{u^5 + B^2 u^2} f(u) a_1^A}{\sqrt{1 + f(u)(a_1^A)^2 - (a_0^V)^2 + f(u)u^3 x_4'^2}} = j_A - \frac{3}{2} B\mu + 3Ba_0^V, \quad (2.5)$$

$$\frac{\sqrt{u^5 + B^2 u^2} a_0^V}{\sqrt{1 + f(u)(a_1^A)^2 - (a_0^V)^2 + f(u)u^3 x_4'^2}} = d - \frac{3}{2} Ba_1^A(\infty) + 3Ba_1^A. \quad (2.6)$$

The corresponding density and current density, d, j_A , at the boundary ($u \rightarrow \infty$) are defined as

$$j^\mu(x, u \rightarrow \infty) \equiv \left. \frac{\delta S_{eom}}{\delta A_\mu} \right|_{u \rightarrow \infty} \quad (2.7)$$

$$\equiv (d, \vec{j}_A). \quad (2.8)$$

They are related to the components of the U(1) gauge field by

$$d = \left. \frac{\sqrt{u^5 + B^2 u^2} a_0^V}{\sqrt{1 + f(u)(a_1^A)^2 - (a_0^V)^2 + f(u)u^3 x_4'^2}} \right|_{\infty} - \frac{3}{2} Ba_1^A(\infty), \quad (2.9)$$

$$j_A = \left. \frac{\sqrt{u^5 + B^2 u^2} f(u) a_1^A}{\sqrt{1 + f(u)(a_1^A)^2 - (a_0^V)^2 + f(u)u^3 x_4'^2}} \right|_{\infty} - \frac{3}{2} B\mu. \quad (2.10)$$

For the phase of pure pion gradient where chiral symmetry is broken, the axial current j_A is set to zero and the density $d = \frac{3}{2} B \nabla \varphi$ is the definition adapted from the Wess-Zumino-Witten action of the boundary gauge theory [7].

The constant of motion with respect to $x_4(u)$ for the pure pion gradient phase yields

$$(x_4'(u))^2 = \frac{1}{u^3 f(u)} \left[\frac{u^3 \left[f(u)(C(u) + D(u)^2) - 9B^2 \left(a_0^V - \frac{\mu}{2} \right)^2 \right]}{F^2} - 1 \right]^{-1}, \quad (2.11)$$

where

$$F = \frac{u_c^3 \sqrt{f(u_c)} \sqrt{f(u_c)(C(u_c) + D(u_c)^2) - 9B^2 \left(a_0^V(u_c) - \frac{\mu}{2}\right)^2} x_4'(u_c)}{\sqrt{1 + f(u_c)u_c^3 x_4'^2(u_c)}} \quad (2.12)$$

$$= u_c^{3/2} \sqrt{f(u_c)C(u_c) - 9B^2 \left(a_0^V(u_c) - \frac{\mu}{2}\right)^2}, \quad (2.13)$$

with $C(u) \equiv u^5 + B^2 u^2$, $D(u) \equiv d - 3B \nabla \varphi / 2 + 3B a_1^A(u)$. u_c is the position where the D8 and $\overline{\text{D8}}$ branes connect. Since there is no instanton in this case, the branes connect smoothly at u_c . We also have $D(u_c) = 0$ from $a_1^A(u_c) = 0$, and $x_4'(u_c) = \infty$.

Since the DBI action, eq. (2.3), is divergent from the limit $u \rightarrow \infty$, we would need the action of the magnetized vacuum for the regularization. For the magnetized vacuum, we can let the non-normalizable modes, $a_0^V, a_1^A = 0$ and $d, j_A = 0$. The vacuum action then takes the following form

$$S[\text{magnetized vacuum}] = \int_{u_0}^{\infty} \sqrt{C(u)(1 + f(u)u^3 x_4'^2)} \Big|_{vac} du,$$

where

$$x_4'(u)|_{vac} = \frac{1}{\sqrt{f(u)u^3 \left(\frac{f(u)u^3 C(u)}{f(u_0)u_0^3 C(u_0)} - 1\right)}}. \quad (2.14)$$

Again, the position of the tip of the brane configuration is denoted by u_0 . The temperature and field dependence of the position u_0 are given in figure 1 of ref. [14]. It saturates approximately at 1.23 for all temperatures at high magnetic field. The action of the vacuum will be used to regulate the infinity of the DBI action from the limit $u \rightarrow \infty$ when we calculate the free energy of the dual gauge matter in the subsequent section.

2.1 Zero temperature approximation $f(u) \simeq 1$

We can numerically solve the equations of motion, eq. (2.5), (2.6) by using the shooting algorithm. However, it is illustrative to consider first the limiting case of zero temperature approximation where $f(u) \simeq 1$ and the equations of motion are sufficiently simplified that they yield exact analytic solutions. Later on we will actually find from the numerical solutions that most physical properties of the pion gradient phase are insensitive to the change of temperature. Interestingly, the bulk theory becomes dual to the Nambu-Jona-Lasinio (NJL) type model in the zero-temperature limit [15].

Starting from the equations of motion, eq. (2.5), (2.6), can be rewritten as

$$a_0^V \left(a_0^V - \frac{\mu}{2}\right) = f(u) a_1^A a_1'^A \quad (2.15)$$

$$f(u) a_0^V a_1'^A = \frac{9B^2 a_1^A \left(a_0^V - \frac{\mu}{2}\right)}{u^5 + B^2 u^2} (1 + f u^3 x_4'^2 + f a_1'^{A2} - a_0^V{}^2). \quad (2.16)$$

From eq. (2.15), for $f = 1$ we can solve to obtain

$$\left(a_0^V - \frac{\mu}{2}\right)^2 - \left(\frac{\mu}{2}\right)^2 = a_1^A{}^2 - (\nabla \varphi)^2. \quad (2.17)$$

Using eq. (2.16), direct integration leads to

$$a_0^V = \frac{\mu}{2} + \sqrt{\left(\frac{\mu}{2}\right)^2 - (\nabla\varphi)^2} \cosh I(u) \quad (2.18)$$

$$a_1^A = \sqrt{\left(\frac{\mu}{2}\right)^2 - (\nabla\varphi)^2} \sinh I(u), \quad (2.19)$$

where

$$I(u) \equiv \int_{u_c}^u du \sqrt{g(u, u_c, B) \left[\frac{C(u)}{9B^2} - \left(\left(\frac{\mu}{2}\right)^2 - (\nabla\varphi)^2 \right) \right]^{-1}}, \quad (2.20)$$

$$g(u, u_c, B) \equiv 1 + u^3 x_4'^2 \quad (2.21)$$

$$= 1 + \left[\frac{u^3(C(u) - 9B^2((\frac{\mu}{2})^2 - (\nabla\varphi)^2))}{u_c^3(C(u_c) - 9B^2((\frac{\mu}{2})^2 - (\nabla\varphi)^2))} - 1 \right]^{-1}, \quad (2.22)$$

by using the boundary conditions $a_1^A(u_c) = 0$ and eq. (2.17) at u_c . Additionally, there are two constraints which need to be satisfied,

$$\cosh I_\infty = \frac{\mu}{2} \frac{1}{\sqrt{\left(\frac{\mu}{2}\right)^2 - (\nabla\varphi)^2}}, \quad (2.23)$$

$$L_0 = 1 = 2 \int_{u_c}^\infty du x_4'(u), \quad (2.24)$$

where $I_\infty \equiv I(u \rightarrow \infty)$. In the zero temperature case x_4' is given by

$$x_4'(u) = \left[u^3 \left(\frac{u^3(C(u) - 9B^2((\frac{\mu}{2})^2 - (\nabla\varphi)^2))}{u_c^3(C(u_c) - 9B^2((\frac{\mu}{2})^2 - (\nabla\varphi)^2))} - 1 \right) \right]^{-1/2}. \quad (2.25)$$

The pion gradient is thus

$$\nabla\varphi = \frac{\mu}{2} \tanh I_\infty. \quad (2.26)$$

In order to obtain the solutions, we numerically solve for u_c from the constraints eq. (2.23) and eq. (2.24) simultaneously by fixing two parameters among $(B, d, \nabla\varphi, \mu)$. The solutions always have $\frac{\mu}{2} > \nabla\varphi$ as a reality condition.

As is found in ref. [10] for the pure pion gradient and ref. [11, 16] for the model with instantons, there are 2 possible brane configurations satisfying the scale fixing condition $L_0 = 1$, one with small and one with large u_c . The brane configuration with small u_c has longer stretch in the u -direction and therefore has higher energy than the configuration with large u_c . The excess energy makes this configuration less preferred thermodynamically. For the pure pion gradient phase, there is also the small- u_c configuration (for sufficiently large μ and small B) which we found to be less preferred thermodynamically even than the vacuum. Therefore this configuration will not be considered in this article.

The solutions can be explored by slicing through the plane in the parameter space at fixed magnetic field (B), fixed density (d), and fixed chemical potential (μ) respectively. At fixed B , the solutions are shown in figure 1 for the position u_c and the chemical potential

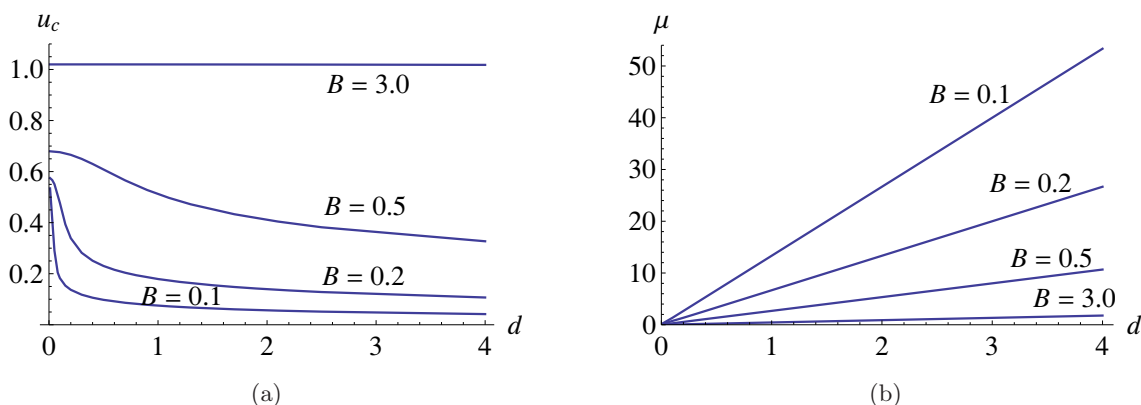


Figure 1. The position u_c (a) and the chemical potential (b) as a function of the density at fixed magnetic field B in the zero temperature limit.

as a function of the density. For small B , the position u_c has certain variation with respect to the density. As B increases, u_c saturates to an almost constant curve with a slight density dependence. The chemical potential at fixed $B(\geq 0.1)$ is found to be an exact linear function of the density. The slope of the linear function is inversely proportional to B . The relation can be summarized into the following simple form

$$\mu = \frac{4}{3} \frac{d}{B} \quad \text{for } B \geq 0.1. \tag{2.27}$$

This implies from $d = 3B\nabla\varphi/2$ that $\mu = 2\nabla\varphi$ for $B \geq 0.1$. The linear relation between μ and d can be interpreted as the absence of self-interaction among the pion gradient excitations. Each pion gradient excitation seems to behave as free entity for $B \geq 0.1$. For small $B < 0.1$, we also find the linear relation between μ and d . It will be shown subsequently that $\mu \sim d/B^2$ for small B in the analysis at fixed μ .

For fixed d , the position u_c and the chemical potential are shown as functions of B in figure 2, 3 for $d = 1.0$. Solutions exist for the entire range of B , down to $u_c(B = 0) = 0$. The chemical potential μ is found to be inversely proportional to B as is shown in figure 3. This is consistent with eq. (2.27).

For fixed μ , figure 4 shows interesting transition between 2 regions of the parameter space. In figure 5, the relation between d and B is shown to be approximately quadratic for $B \leq 0.2$ and linear for $B \gtrsim 0.2$. From $d = 3B\nabla\varphi/2$, this implies that $\nabla\varphi$ is a linear function of B for $B \leq 0.2$ and a constant function for $B \gtrsim 0.2$. Figure 4(b) confirms the behaviour. Since the saturation at large B occurs around $\nabla\varphi = \mu/2$, the slope of the linear region, $B \leq 0.2$, is therefore proportional to μ . Consequently, for small B , $\nabla\varphi \sim \mu B$. The behaviour at small B is similar to the behaviour found in ref. [7, 9] for the confined phase. The result in the deconfined phase of the SS model in the zero temperature limit was first obtained in ref. [10].

It should be noted that the nonlinear effects of the DBI action become apparent for $B \gtrsim 0.2$ where $\nabla\varphi \simeq \mu/2$. From eq. (2.20), (2.26) since $I_\infty \rightarrow \infty$ as $B \rightarrow \infty$, the saturation always occurs at $\nabla\varphi \simeq \mu/2$ for any μ . As B increases, the pion gradient does not change

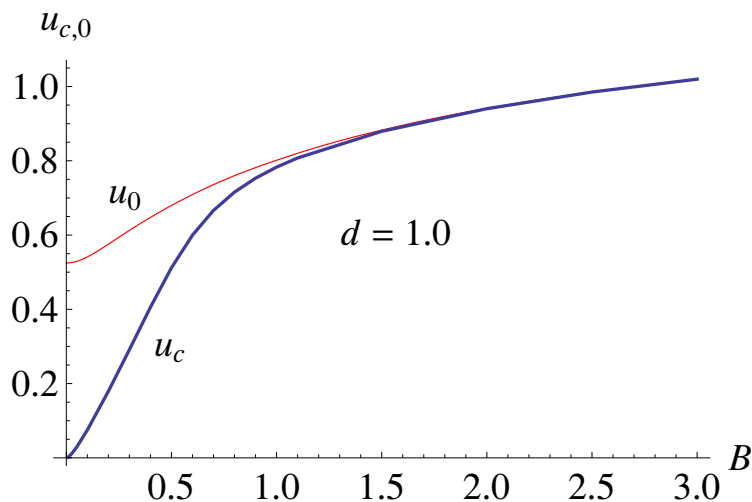


Figure 2. Position u_c as a function of B at a fixed density $d = 1.0$ in the zero temperature limit, the position u_0 of the magnetized vacuum is shown for comparison.

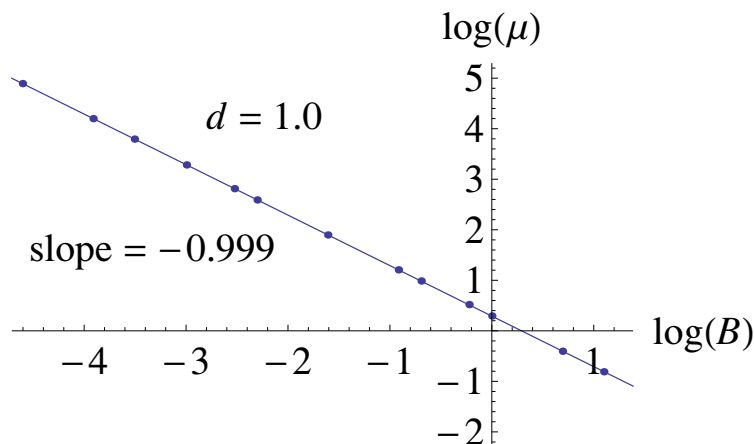


Figure 3. Chemical potential as a function of B at $d = 1.0, T = 0$ in the logarithmic scale.

but its baryonic density increases linearly with the field. This $\nabla\varphi$ -saturation is a new effect observed only in the theory with DBI gauge interaction.

3 Thermodynamical properties of the pure pion gradient phase

In the pure pion gradient phase, since $x'_4 \rightarrow \infty$ at u_c , the integrand of the action diverges at u_c in addition to the limit $u \rightarrow \infty$. This also occurs with the magnetized vacuum where x'_4 is divergent at u_0 . However, the limit which makes the integral and consequently the action divergent comes only from $u \rightarrow \infty$ (the divergences at $u_{0,c}$ are weaker than a simple pole and thus finite over integration). We can therefore regulate the action by subtracting the total action with the action of the magnetized vacuum in the usual manner.

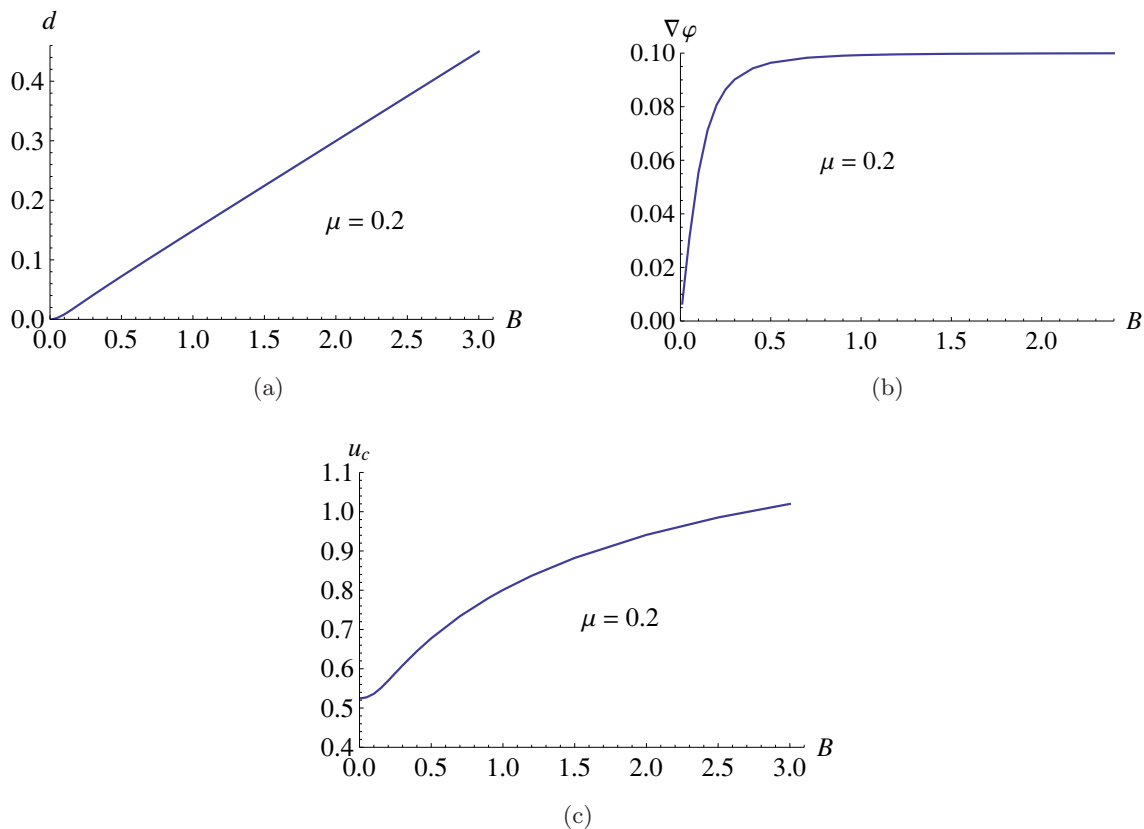


Figure 4. The density (a), the pion gradient (b), and the position u_c (c) as a function of B at fixed $\mu = 0.2, T = 0$.

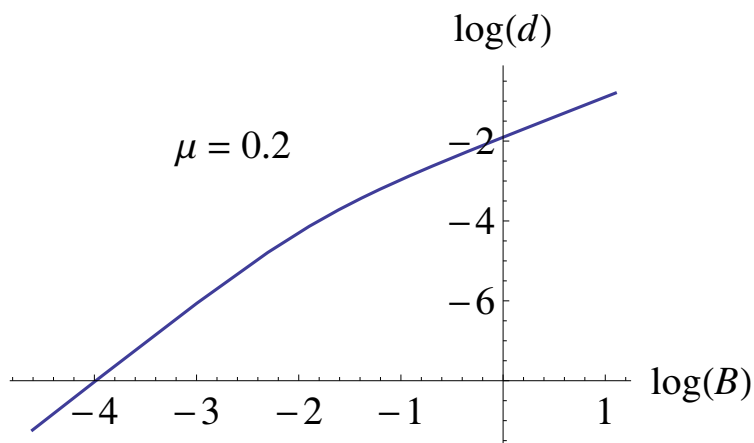


Figure 5. The density as a function of B at $\mu = 0.2, T = 0$ in the logarithmic scale.

Generically, the free energy can be defined at fixed density (in the canonical ensemble) or fixed chemical potential (in the grand canonical ensemble), they are related by the Legendre transform. In the holographic model, the free energy of the dual gauge matter at a fixed chemical potential is proportional to action of the D8-branes. Therefore, the

regulated free energy in the canonical ensemble (Helmholtz free energy) is given by

$$\mathcal{F}_E(d, B) = \Omega(\mu, B) + \mu d, \quad (3.1)$$

where $\Omega(\mu, B) = S[a_0(u), a_1(u)](e.o.m.) - S[\text{magnetized vacuum}] \equiv \mathcal{F}(\mu, B)$, the free energy in the grand canonical ensemble (also known as the grand potential or Landau free energy).

We can calculate the total action satisfying the equation of motion $S[a_0(u), a_1(u)](e.o.m.) = S_{D8} + S_{CS}$ to be

$$S_{D8} = \mathcal{N} \int_{u_c}^{\infty} du C(u) \sqrt{\frac{f(u)(1 + f(u)u^3x_4'^2)}{f(u)(C(u) + D(u)^2) - 9B^2\left(a_0^V - \frac{\mu}{2}\right)^2}}, \quad (3.2)$$

$$S_{CS} = -\mathcal{N} \frac{3}{2} B \int_{u_c}^{\infty} du \frac{\left(3Ba_0^V\left(a_0^V - \frac{\mu}{2}\right) - f(u)D(u)a_1^A\right) \sqrt{\frac{1}{f(u)} + u^3x_4'^2}}{\sqrt{f(u)(C(u) + D(u)^2) - 9B^2\left(a_0^V - \frac{\mu}{2}\right)^2}}. \quad (3.3)$$

For zero temperature the total action reduces to

$$S_{e.o.m.} = \mathcal{N} \int_{u_c}^{\infty} du \sqrt{\frac{g(u, u_c, B)}{C(u) - 9B^2\left(\left(\frac{\mu}{2}\right)^2 - (\nabla\varphi)^2\right)}} \left(C(u) - \frac{9B^2}{2} \left(\frac{\mu}{2} a_0^V(u) - (\nabla\varphi)^2\right)\right).$$

We can compute this action by substituting eq. (2.18) into the expression. The free energy at fixed chemical potential $\mathcal{F}(\mu, B)$ of the pure pion gradient phase at zero temperature is shown in figure 6. Once $d, \mu > 0$, the free energy becomes smaller than the free energy of the magnetized vacuum (being negative) and thus thermodynamically preferred than the vacuum phase. The magnetization at fixed chemical potential $\mathcal{M}(\mu, B) = -\frac{\partial\mathcal{F}(\mu, B)}{\partial B}$ therefore increases from zero and becomes constant $M(\mu = 0.2, B) \simeq 0.0152$ at large field ($B > 0.2$) as we can see from the slope of figure 6. On the other hand, the magnetization at fixed $d = 1.0$, $M(d, B) = -\frac{\partial\mathcal{F}_E(d, B)}{\partial B}$, of the pure pion gradient phase is a rapidly decreasing function of B as is shown in figure 7.

The pressure of the pure pion gradient as a function of the density can be calculated using eq. (2.27) and $d = \frac{\partial P}{\partial \mu}$ (see ref. [17]),

$$P(d, B) = \mu(d, B)d - \int_0^d \mu(d', B) d(d'), \quad (3.4)$$

$$= \frac{1}{2} k(B) d^2, \quad (3.5)$$

where $k(B) = 4/3B$ for $B \geq 0.1$. The quadratic dependence of the pressure on the density without higher order term reveals that the pion gradient excitations behave like free particles without either repulsive or attractive interaction among themselves.

For the parameter space in the region $d \ll 1, B \ll 1$ such as the regions shown in figure 4, 5, since $\nabla\varphi \sim \mu B, d = 3B\nabla\varphi/2$, we have $d = \alpha\mu B^2$ for some constant α . In this case, the linear relations between μ and d is still valid and the equation of state is again given by eq. (3.5) with $k(B) = 1/\alpha B^2$ (for $\mu = 0.2, \alpha \simeq 4.634$). This behaviour is similar

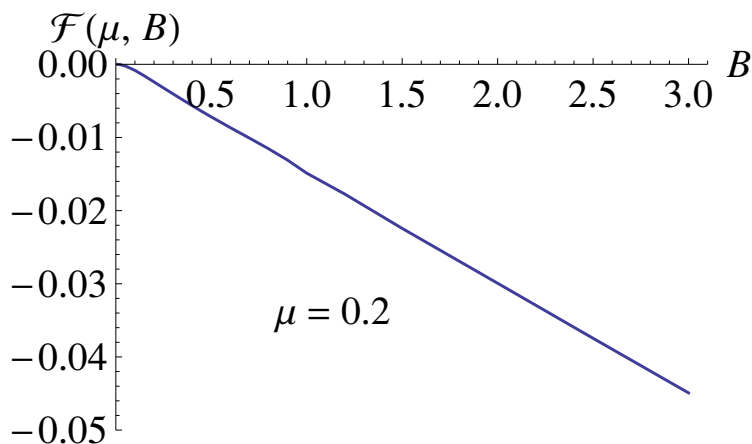


Figure 6. The Landau free energy as a function of B at fixed $\mu = 0.2, T = 0$.

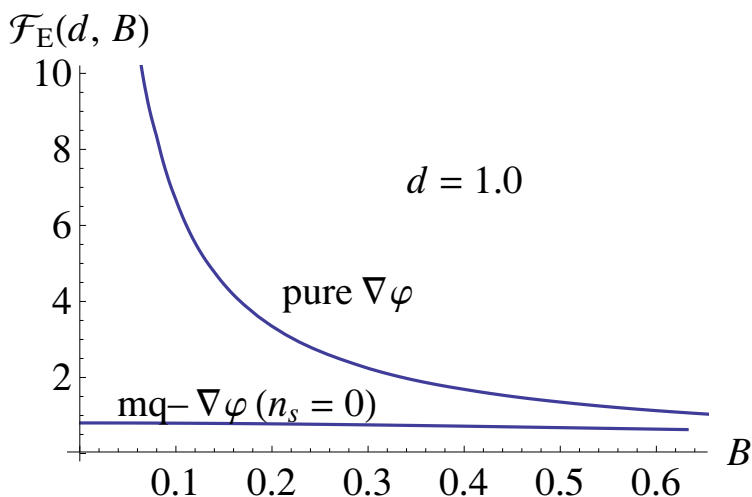


Figure 7. The Helmholtz free energy as a function of the density of the pure pion gradient phase compared with the multiquark- $\nabla\varphi$ phase at fixed $d = 1.0, T = 0$. The number of colour strings n_s represents the colour charges of the multiquark in unit of $1/N_c$. Baryon corresponds to multiquark with $n_s = 0$.

to what found in ref. [7] using the Wess-Zumino-Witten term in the boundary theory and in ref. [9, 10] for the confined and deconfined SS model at zero temperature.

The energy density can be calculated straightforwardly

$$\rho = \int_0^d \mu(\eta, B) d\eta, \tag{3.6}$$

$$= \frac{1}{2}k(B)d^2, \tag{3.7}$$

where $k(B) = 1/\alpha B^2, 4/3B$ for small and large B respectively. The results are remarkably similar to the results from the bottom-up AdS/QCD model considered in ref. [8]. The equation of state then becomes simply $P = \rho$ representing free gas of the solitonic excita-

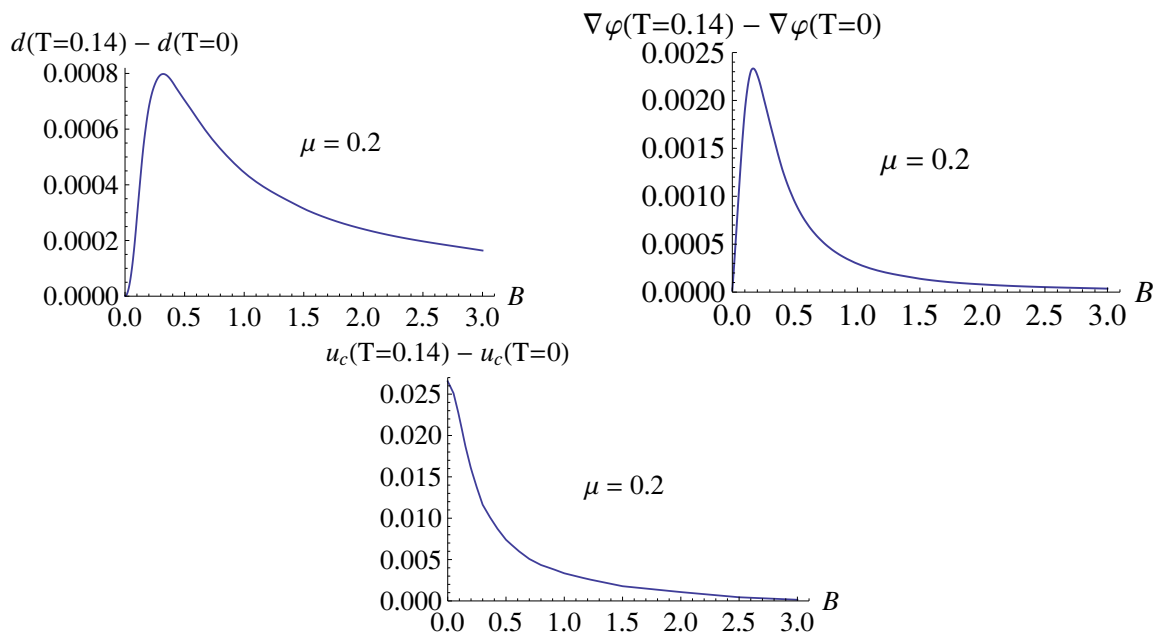


Figure 8. The difference between the density, the pion gradient, and the position u_c of the $\nabla\varphi$ phase at $T = 0.14$ and $T = 0$ as a function of B for $\mu = 0.2$.

tions of the the pion gradient. The adiabatic index, Γ , and the sound speed, c_s , are then calculated to be

$$\Gamma \equiv \frac{\rho}{P} \frac{\partial P}{\partial \rho} = \frac{\rho}{P} c_s^2 = 1, \quad (3.8)$$

$$c_s = 1, \quad (3.9)$$

the typical behaviour of the free gas.

For nonzero temperature, the full equations of motion, eq. (2.5), (2.6) can be solved numerically by double shooting algorithm aiming for two conditions to be satisfied at once: $a_1^A(u_c) = 0, L_0 = 1$ (with x_4' from eq. (2.11)) while fixing B, μ and d (and consequently $\nabla\varphi$). The boundary conditions, $a_0^V(\infty) = \mu, a_1^A(\infty) = \nabla\varphi$, are adjusted until we hit the target conditions. It is found that the temperature dependence of every physical quantity of the pure pion gradient is very weak. Figure 8 shows the *difference* of the density, the pion gradient, and the position u_c at fixed $\mu = 0.2$ between $T = 0.14$ and $T = 0$. Observe that the difference in the temperature dependence of the density and the pion gradient are the most distinctive in the transition region when the magnetic field changes from small to large values.

3.1 Comparison to the multiquark- $\nabla\varphi$ phase

We would like to consider whether the pure pion gradient phase is thermodynamically preferred than the other nuclear phases in certain regions of the parameter space. In the deconfined SS model in the presence of the magnetic field, there are generically 3 possible phases in addition to the vacuum; the chiral symmetric QGP phase, the chirally

broken phase of multiquark- $\nabla\varphi$ (MQ- $\nabla\varphi$), and the pure pion gradient ($\nabla\varphi$) phase. The multiquark nuclear phase has been studied in ref. [11, 14, 18] and found to be the most preferred phase for the dense deconfined nuclear matter under moderate external magnetic fields. The multiquark phase actually has certain mixture of the pion gradient as the source for the baryon density. This is inevitable since the response of the nuclear matter to the external magnetic field is in the form of the spatial variation of the chiral condensate in the direction of the applied field which we call the pion gradient.

However, the ratio of the pion gradient population with respect to the multiquark decreases as d grows [14]. It is thus suggestive that the multiquark phase is likely to be more thermodynamically preferred than the pion gradient phase. In this subsection we directly compare the two phases at zero temperature using the free energy at fixed density $d = 1.0$. The MQ- $\nabla\varphi$ phase imposes the boundary conditions (see ref. [11, 14] for details);

$$j_A = 0, \quad a_1^A(u_c) = 0, \quad a_0^V(u_c) = \frac{1}{3}u_c\sqrt{f(u_c)} + n_s(u_c - u_T),$$

where n_s is the number of colour strings (hanging from the baryon vertex down to the horizon) in fractions of $1/N_c$.

The result is shown in figure 7. Clearly, the multiquark-pion gradient (MQ- $\nabla\varphi$) phase is more preferred than the pure pion gradient phase. Similar behaviours are confirmed for small $d \simeq 0.1$ and large $d \gg 1$. Especially at large densities, since the baryon chemical potential of the MQ- $\nabla\varphi$ phase increases slower than a linear function [11] whilst it is linear for the $\nabla\varphi$ phase, the dominant term μd in the free energy for the MQ- $\nabla\varphi$ phase becomes much smaller and thus more stable thermodynamically.

However, there is a region of parameter space where the $\nabla\varphi$ phase is dominant. When the baryon chemical potential $\mu < \mu_{\text{onset}} \equiv \mu(d = 0) = \frac{1}{3}u_0\sqrt{f(u_0)} + n_s(u_0 - u_T)$ of the multiquark, the multiquarks cease to exist and the pion gradient which can be constructed at arbitrarily small μ (since $\mu \sim d$) will be dominating. The corresponding transition line in the (μ, T) diagram for $B = 0$ is shown in figure 8 of ref. [18]. For $B > 0$, dependence of u_0 on B affects the transition line accordingly as shown in figure 9. The dotted line represents schematic transition to the chiral symmetric quark-gluon plasma (χS -QGP) phase. The chiral symmetry restoration between the magnetized vacuum and the χS -QGP has been studied in ref. [19]. The transition between the pure pion gradient phase and the χS -QGP has been explored in ref. [10] with $f = 1$ approximation for the pure pion gradient. Since we found that the $\nabla\varphi$ phase is insensitive to the change of temperature, the results in ref. [10] should be justified to be a good approximated phase diagram. The chiral symmetry restoration between the MQ- $\nabla\varphi$ phase and the χS -QGP phase has been investigated in ref. [14].

4 Conclusions and discussions

The behaviour of the chirally broken pure pion gradient phase in the deconfined SS model is studied in the zero temperature limit and subsequently at finite temperature. The magnetic response of the chirally broken phase is linear $\nabla\varphi \sim \mu B$ for small field and saturates to constant value $\nabla\varphi \sim \mu/2$ for large field.

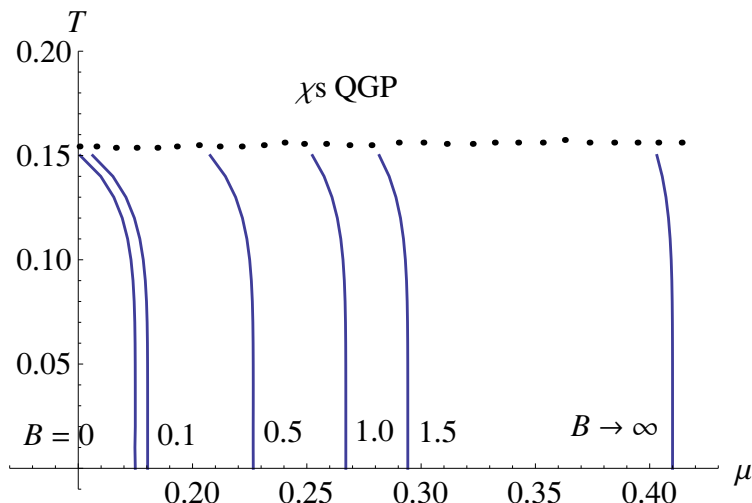


Figure 9. The onset chemical potential of the multiquark- $\nabla\varphi$ phase as a function of T, B (for $B \rightarrow \infty, u_0 = 1.23$ is used). These lines can be served as the transition lines between the $\nabla\varphi$ phase on the left and multiquark- $\nabla\varphi$ phase ($n_s = 0$) on the right. The dotted line represents schematic transition to the chiral symmetric QGP phase.

Relationship between μ and d is also linear $\mu = k(B)d$ where $k(B) \sim 1/B^2, 1/B$ for small and large B respectively. This implies that the excitations of the pion gradient behave like a free gas with no interaction among each other. The equation of state is thus simply $P = \rho$ with the sound speed equal to the speed of light. The free energies at fixed μ and d are obtained numerically. Magnetization at fixed μ increases with B for small field and drops to constant value for large field. Magnetization at fixed d is a decreasing function with respect to the magnetic field.

Using the free energy at fixed density, we show that the pure $\nabla\varphi$ phase is less preferred thermodynamically than the MQ- $\nabla\varphi$ phase at zero temperature. The configuration of the pure pion gradient phase is found to be insensitive to the change of temperature, the difference of the free energy at fixed μ for $T = 0$ and $T = 0.14$ is minimal, only about $\lesssim 2 \times 10^{-4}$. On the other hand, the free energy of the MQ- $\nabla\varphi$ phase is a decreasing function in the temperature [14]. Therefore, we can conclude that the pure pion gradient phase is generically less preferred than the MQ- $\nabla\varphi$ for general situation.

However, there is an exception for small chemical potential, $\mu \simeq 0.175 - 0.41$. When $\mu < \mu_{\text{onset}}$ of the multiquarks, the multiquarks simply cannot exist while the pion gradient can be induced at arbitrarily small μ . Therefore, in this region of the parameter space, the pure pion gradient phase is dominating over any other phases. The transition lines are given by $\mu = \mu_{\text{onset}}$ in the (μ, T) plane. The interior of certain classes of the dense astrophysical objects such as the magnetars [20] would have the corresponding regions where the chemical potential (and the density) and temperature fall into this range. In those regions, the dominating nuclear phase which governs physics of the stars would be the pure pion gradient.

Finally, the conversion factors to the corresponding physical quantities in the natural unit ($\hbar = c = 1$) are the following (see e.g. ref. [9], we have set $R_{D4} = 1$ in this article):

$1/2\pi\alpha'$ for B , $R_{D4}/2\pi\alpha'$ for μ , $2\pi\alpha'\mathcal{N}/R_{D4}$ for d , and $R_{D4}^2 f_\pi/2\pi\alpha'$ for $\nabla\varphi$ where f_π is the pion decay constant. For the magnetic field, the conversion factor $1/2\pi\alpha'$ with $\alpha'^{-1} = 0.2 \text{ GeV}^2$ corresponds to approximately 5.37×10^{14} Tesla in the SI unit.

Acknowledgments

P.B. would like to thank CERN Theoretical Physics Division for the warm hospitality during my visit where this work is completed. P.B. is supported in part by the Thailand Research Fund (TRF) and Commission on Higher Education (CHE) under grant RMU5380048, the Toray Science Foundation, Japan (TSF) and Thailand Center of Excellence in Physics (ThEP). P.B. and T.C. are supported in part by the 90th Year Chulalongkorn Scholarship.

Open Access. This article is distributed under the terms of the Creative Commons Attribution Noncommercial License which permits any noncommercial use, distribution, and reproduction in any medium, provided the original author(s) and source are credited.

References

- [1] J.M. Maldacena, *The large- N limit of superconformal field theories and supergravity*, *Int. J. Theor. Phys.* **38** (1999) 1113 [*Adv. Theor. Math. Phys.* **2** (1998) 231] [[hep-th/9711200](#)] [[SPIRES](#)].
- [2] E. Witten, *Anti-de Sitter space and holography*, *Adv. Theor. Math. Phys.* **2** (1998) 253 [[hep-th/9802150](#)] [[SPIRES](#)].
- [3] O. Aharony, S.S. Gubser, J.M. Maldacena, H. Ooguri and Y. Oz, *Large- N field theories, string theory and gravity*, *Phys. Rept.* **323** (2000) 183 [[hep-th/9905111](#)] [[SPIRES](#)].
- [4] T. Sakai and S. Sugimoto, *Low energy hadron physics in holographic QCD*, *Prog. Theor. Phys.* **113** (2005) 843 [[hep-th/0412141](#)] [[SPIRES](#)].
- [5] T. Sakai and S. Sugimoto, *More on a holographic dual of QCD*, *Prog. Theor. Phys.* **114** (2005) 1083 [[hep-th/0507073](#)] [[SPIRES](#)].
- [6] O. Aharony, J. Sonnenschein and S. Yankielowicz, *A holographic model of deconfinement and chiral symmetry restoration*, *Annals Phys.* **322** (2007) 1420 [[hep-th/0604161](#)] [[SPIRES](#)].
- [7] D.T. Son and M.A. Stephanov, *Axial anomaly and magnetism of nuclear and quark matter*, *Phys. Rev. D* **77** (2008) 014021 [[arXiv:0710.1084](#)] [[SPIRES](#)].
- [8] E.G. Thompson and D.T. Son, *Magnetized baryonic matter in holographic QCD*, *Phys. Rev. D* **78** (2008) 066007 [[arXiv:0806.0367](#)] [[SPIRES](#)].
- [9] O. Bergman, G. Lifschytz and M. Lippert, *Magnetic properties of dense holographic QCD*, *Phys. Rev. D* **79** (2009) 105024 [[arXiv:0806.0366](#)] [[SPIRES](#)].
- [10] F. Preis, A. Rebhan and A. Schmitt, *Inverse magnetic catalysis in dense holographic matter*, *JHEP* **03** (2011) 033 [[arXiv:1012.4785](#)] [[SPIRES](#)].
- [11] P. Burikham, *Magnetic properties of holographic multiquarks in the quark-gluon plasma*, *JHEP* **04** (2010) 045 [[arXiv:0909.0614](#)] [[SPIRES](#)].

- [12] E. Witten, *Anti-de Sitter space, thermal phase transition and confinement in gauge theories*, *Adv. Theor. Math. Phys.* **2** (1998) 505 [[hep-th/9803131](#)] [[SPIRES](#)].
- [13] K.-Y. Kim, S.-J. Sin and I. Zahed, *Dense hadronic matter in holographic QCD*, [hep-th/0608046](#) [[SPIRES](#)].
- [14] P. Burikham, *Magnetic Phase Diagram of Dense Holographic Multiquarks in the quark-gluon Plasma*, *JHEP* **05** (2011) 121 [[arXiv:1103.4379](#)] [[SPIRES](#)].
- [15] E. Antonyan, J.A. Harvey, S. Jensen and D. Kutasov, *NJL and QCD from string theory*, [hep-th/0604017](#) [[SPIRES](#)].
- [16] O. Bergman, G. Lifschytz and M. Lippert, *Holographic Nuclear Physics*, *JHEP* **11** (2007) 056 [[arXiv:0708.0326](#)] [[SPIRES](#)].
- [17] P. Burikham, E. Hirunsirisawat and S. Pinkanjanarod, *Thermodynamic Properties of Holographic Multiquark and the Multiquark Star*, *JHEP* **06** (2010) 040 [[arXiv:1003.5470](#)] [[SPIRES](#)].
- [18] P. Burikham, A. Chatrabhuti and E. Hirunsirisawat, *Exotic Multi-quark States in the Deconfined Phase from Gravity Dual Models*, *JHEP* **05** (2009) 006 [[arXiv:0811.0243](#)] [[SPIRES](#)].
- [19] C.V. Johnson and A. Kundu, *External Fields and Chiral Symmetry Breaking in the Sakai-Sugimoto Model*, *JHEP* **12** (2008) 053 [[arXiv:0803.0038](#)] [[SPIRES](#)].
- [20] R.C. Duncan and C. Thompson, *Formation of very strongly magnetized neutron stars-implications for gamma-ray bursts*, *Astrophys. J.* **392** (1992) L9 [[SPIRES](#)].